7. SUMMARY[1]

Shipboard Scientific Party[2]

INTRODUCTION

Leg 172 achieved or exceeded nearly all of the objectives outlined in the cruise prospectus. At most of the sites (Fig. 1) sedimentation has been continuous and at a high deposition rate throughout the Pleistocene, and important features of ocean and climate change such as the evolution of the "100-k.y. world" from the "40-k.y. world" are evident. Most shipboard work is preliminary and concentrated on identifying evidence for orbital-scale climate changes, but millennial- and perhaps centennial-scale changes should be resolvable at some sites. At a few sites, the recovered sequences extend to the middle Pliocene, providing material for study of climate changes associated with the origin of Northern Hemisphere glaciation. Nearly all sites contained useful records of the behavior of the Earth's magnetic field, and many of these contain high-resolution records with previously unseen field variability. Preliminary micropaleontological results suggest that some widely accepted datum levels may not be applicable in the western North Atlantic, and the dating of others may be more precisely fixed. Finally, shipboard geochemical results have documented the important role of organic and inorganic diagenesis in the sediment drift environment.

Current control on sedimentation is obvious at all locations, so shore-based research will provide the opportunity to link together sedimentological, micropaleontological, and geochemical proxy data for ocean circulation and climate change. Indeed, the influence of thermohaline circulation is so pervasive in the western North Atlantic that it accounts for much of the uniformity observed among coring locations spanning a depth range in excess of 4 km. This is the first "theme" to be discussed in the following sections. A second theme will be depth-dependent variability among shipboard measurements. These will be followed by evidence for the "40-k.y." to "100-k.y." transition in climate, preliminary paleomagnetic results, preliminary biostratigraphic results, and preliminary results on the geographic extent of gas hydrate.

UNIFORMITY OF REGIONAL SEDIMENTATION

One intriguing result from Leg 172 is the discovery that nearly identical sedimentary units are present from the shallowest site on the Carolina Slope (Site 1054, 1291 m) to the deepest site on the Blake-Bahama Outer Ridge (BBOR; Site 1062, 4775 m; Fig. 2). Every location has an upper unit marked by cyclic alternation between nannofossil-rich and clay-rich sediments (Unit I). At locations where a hole penetrated deep enough, it appears that the base of Unit I is close to or a little older than the Brunhes/Matuyama (B/M) boundary, roughly 800 ka (Site 1055 is an exception, with the base of Unit I at ~500 ka). That this lithological change is close in age to the middle Pleistocene origin of 100-k.y. orbital forcing of climate (~900 ka) attests to the strong influence of climate on sedimentation and ocean circulation. A clay-rich Unit II has been identified at most of these sites, but the age of its base differs among them, and the extent of the underlying mixed sediments of Unit III is unknown. The three subunits of the Bermuda Rise seem to be correlative to the three units of the BBOR (Fig. 2), although they differ in important details, such as significant abundance of opal in Unit I at the Bermuda Rise. This similarity indicates that patterns of sedimentation are basinwide.

Stratigraphic coherence among Leg 172 sites is evident on much shorter time and depth scales. In the absence of oxygen isotope stratigraphy for Leg 172 sites, a preliminary chronology has been determined for the past 900 k.y. using magnetic susceptibility records at all locations except Sites 1054 and 1064 (Fig. 3). As at many other North Atlantic locations, magnetic susceptibility is a proxy for oxygen isotope or percent carbonate values, with higher magnetic susceptibility during glacial stages because of increased terrigenous flux to the ocean. Such a pattern is evident at most BBOR locations and to some degree at the Bermuda Rise (Site 1063) as well, although the pattern is complicated there by diatom accumulation during glacial stages and stadial events. Surprisingly, rates of sedimentation calculated using the chronology based on magnetic susceptibility show few systematic changes on orbital time scales (Fig. 4). For example, with the exception of marine isotope Stages (MISs) 2–4, there is no general trend toward higher rates of sedimentation during glaciation. This may reflect the different bathymetric and hydraulic settings of each site, as well as errors in the age model. But the robust trend toward greater deposition during the past 60 k.y. is consistent from site to site and it is more than can be accounted for by high sediment porosity. It could signify increased continental erosion during the latest glacial–interglacial cycle, possibly coupled with more energetic deep ocean circulation.

The occurrence of "brick-red lutites" is another remarkable feature of the sediments at Sites 1055–1063 (Fig. 5). These hematite-rich sediments are derived from the Permo-Carboniferous deposits of the Canadian Maritime provinces and are transported by glaciers to the Nova Scotian continental margin. From there they are eroded and transported southwestward by deep, recirculating gyres and the Deep Western Boundary Current (DWBC). Using the shipboard "Milankovitch" age model (Fig. 3), a preliminary comparison of red lutite occurrence among the BBOR and Bermuda Rise sites shows they are regionally correlatable and generally deposited during glacial epochs. However, the lithostratigraphic value of the red lutites as well as their possible value as advective proxies for deep circulation are restricted by our limited understanding of the formative diagenetic processes (Barranco et al., 1989). For example, the less common occurrence of red lutites above ~3500 m may mean that DWBC transport is less effective at shallower depths during glaciation, or it may simply mean that red oxidized sediments have been reduced to green or gray sediments.

DEPTH-DEPENDENT VARIABILITY AMONG LEG 172 SITES

Just as many Leg 172 sites have features in common, there are also important differences that stem from factors such as the varying strength of the DWBC at various water depths, increased carbonate dissolution with increased water depth, distance of the site from shore, and others. From shallow sites on the Carolina Slope to the deep BBOR sites, sedimentation rates increase, reaching average late Pleistocene values in excess of 20 cm/k.y. at Sites 1060 and 1061

[1]Keigwin, L.D., Rio, D., Acton, G.D., et al., 1998. *Proc. ODP, Init. Repts.*, 172: College Station, TX (Ocean Drilling Program).

[2]Shipboard Scientific Party is given in the list preceding the Table of Contents.

Prior Chapter Contents Next Chapter

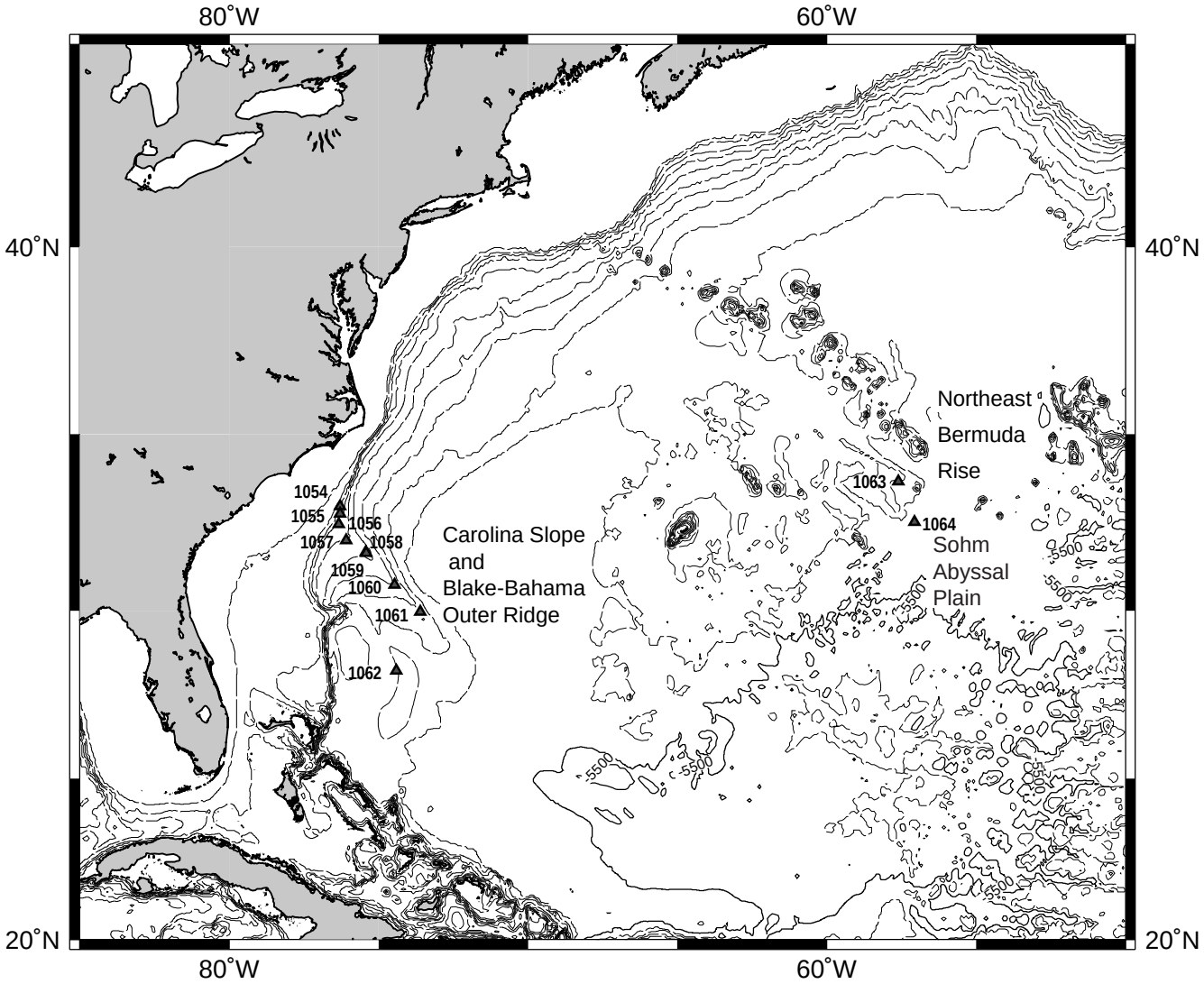

Figure 1. Locations of Leg 172 sites.

(Fig. 4). Sedimentological evidence indicates higher detrital input to the deep sites in the late Pleistocene, again suggesting increased erosion on land and more energetic deep ocean circulation. When $CaCO_3$ accumulation rates are calculated from bulk density and rates of sedimentation, a significant decrease in the average carbonate flux with increasing water depth is found (Fig. 6). The shallowest sites (Sites 1056–1058) appear to have average carbonate fluxes in the 3–4 g/cm^2/k.y. range, whereas the deeper Sites 1061–1063 generally have varying carbonate fluxes from 1–2 g/cm^2/k.y. Despite the lower values on average at the deeper sites, they contain frequent interglacial "spikes" of the highest carbonate fluxes observed in the entire western North Atlantic region. This is not a simple artifact of resolving brief events better in sites with higher deposition rates, because sedimentation rates are equally high at Site 1058, but brief maxima are not evident. A likely explanation for this observation is that the deeper sites are subject to both greater dilution and carbonate dissolution during glacial epochs.

Pore-water chemistry profiles also change with water depth. At all the sites, the chemical composition of interstitial waters is predominantly controlled by early diagenesis associated with microbial decomposition of organic matter (e.g., Berner, 1980; Pedersen and Shimmield, 1991). Except at Site 1054, where an oxidation zone of 8 m thickness was observed, the onset of sulfate reduction at all the sites is close to the seafloor (Fig. 7). In the sulfate reduction zone sulfate concentrations decrease from near-seawater values to <1 mM at the top of the methanogenesis zone. The depth of the sulfate/methane boundary is variable and appears to be controlled by a combination of interrelated factors, such as sedimentation rate, organic carbon content and type, and the upward methane flux. The interface is generally deeper at the deep-water sites of the BBOR (Holes 1062B, 1062E, and 1062H), Bermuda Rise (Site 1063) and Sohm Abyssal Plain (Site 1064), where sedimentation rates and organic contents are relatively low (Fig. 7). Carolina Slope Site 1054 once again is an exception, having a deep sulfate/methane boundary at 48 mbsf. The deep sulfate zone at this site is most likely caused by the relatively low sedimentation rates for the upper part of the sediment column. Pore-water alkalinity production also decreases with increasing water depth (Fig. 7), as do ammonia and phosphate (not shown). This is largely because of the higher organic carbon (and carbonate carbon in the case of alkalinity) fluxes in the upper part of the sediment column.

Other chemical species in pore water show consistent changes associated with sulfate reduction, including Ca and Mg, which are involved in dolomite precipitation, Fe and Mn, which are involved in iron sulfide staining and pyrite formation, and interstitial potassium. Potassium profiles show a downhole increase at the Carolina Slope sites, suggesting replacement by ammonium at clay-mineral exchange sites as the concentration of ammonium builds up in the lower

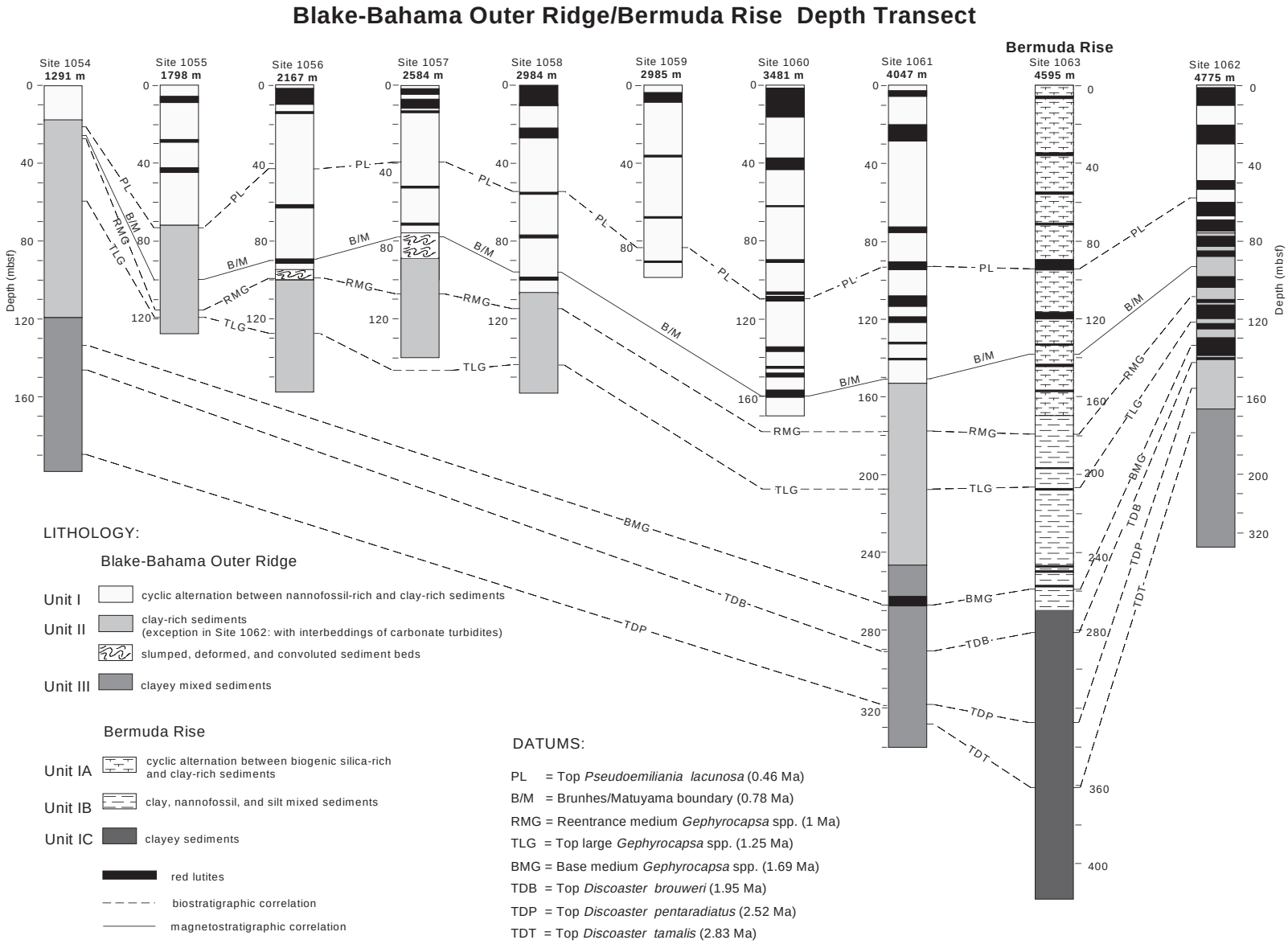

Figure 2. Generalized lithostratigraphy, biostratigraphy, and magnetostratigraphy of Leg 172 sites, except Site 1064. Note the similar sequence of units at all sites. As discussed in the text, this most likely reflects coherent variation of sediment distribution by deep ocean currents basinwide through the late Pliocene and Pleistocene.

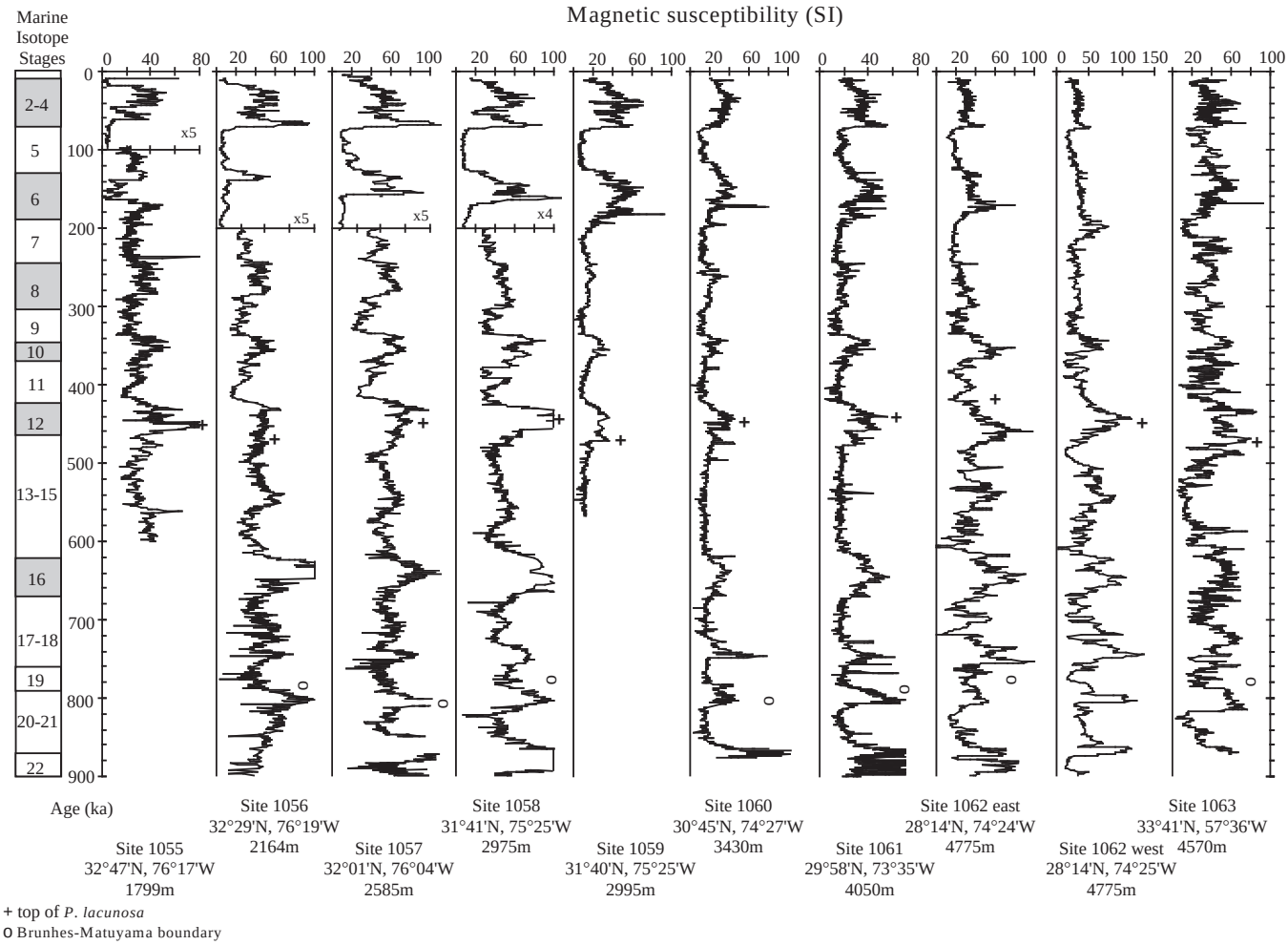

Figure 3. Magnetic susceptibility plotted vs. age for the last 0.9 m.y. of all Leg 172 sites, except Sites 1054 and 1064, where a systematic pattern of magnetic susceptibility was not evident. However, at the remaining sites high magnetic susceptibility is clearly associated with episodes of Pleistocene glaciation. That relationship has been used to assign a chronology based on marine oxygen isotope stages to Sites 1055 through 1063, and is consistent with available biostratigraphic and magnetostratigraphic data for the late Pleistocene. + = last occurrence of *P. Lacunosa*; o = B/M boundary. Note scale of abcissa by a factor of 4 or 5 at Sites 1055 through 1058.

part of the sediment column (Fig. 7; e.g., Rosenfeld, 1979; Mackin and Aller, 1984). However, at deep-water sites on BBOR and Bermuda Rise the potassium concentrations decrease with depth, probably caused by adsorption onto clay minerals in the absence of strong competition by ammonium ions. Interstitial-water silica concentrations increase downhole at sites on the Carolina Slope and BBOR at intermediate water depths, probably conforming with the downhole increase in alkalinity. However, high interstitial-water silica concentrations (>800 mM) in the deep water sites (e.g., upper part of sediment column at Site 1063) generally reflect dissolution of biogenic silica in the sediments.

Downhole variations in methane concentration show a bimodal trend, which indicates that methane enrichment occurs in two distinct depth zones. These zones are shallower in shallow sites, and approximately 80 m deeper in the deep ones (Fig. 8). This probably corresponds to a vertical shift in the sulfate reduction zone from the Carolina Slope to the BBOR and Bermuda Rise locations. At the shallow Site 1054, however, the depth of the onset of methane production is deeper than at the other shallow sites, which may be related to low sedimentation rates in the upper part of the sediment column at this site.

The origin of downhole methane can be inferred from downhole profiles of its ratio to ethane (C_1/C_2). All Leg 172 sites have the same pattern of C_1/C_2 ratio vs. depth, and show a slight decrease from surficial to deep sediment layers (Fig. 9). Values stay higher than 100 in each location, which clearly indicates that methane is mostly of biogenic origin and the end-product of microbial activity. However, the downhole decrease of methane to ethane ratios tends to be more pronounced for shallow sites (Fig. 9, open circles), which indicates a greater increase in ethane contribution with depth. Extrapolation of this trend would indicate C_1/C_2 values lower than 100 by about 300 mbsf, which could herald an increasing contribution of thermogenic hydrocarbons and perhaps more hazardous drilling conditions.

THE 40-K.Y. TO 100-K.Y. TRANSITION: THE MID-PLEISTOCENE CLIMATIC REVOLUTION

Most Leg 172 cores were drilled deep enough to recover the last occurrence (LO) of large *Gephyrocapsa* spp. (dated to 1.25 Ma; Fig. 2) so that the "40-k.y." world of the early Pleistocene would be adequately represented for detailed study. The transition at ~800–900 ka from climate records dominated by a 40-k.y. period to those dominated by the familiar late Pleistocene glaciations that occurred at ~100-k.y. periods is a subject of active research. Evidence for this climate change may be found throughout the western North Atlantic region in the form of a change in lithology (discussed above) and in proxy records such as carbonate accumulation (Fig. 6). Striking evi-

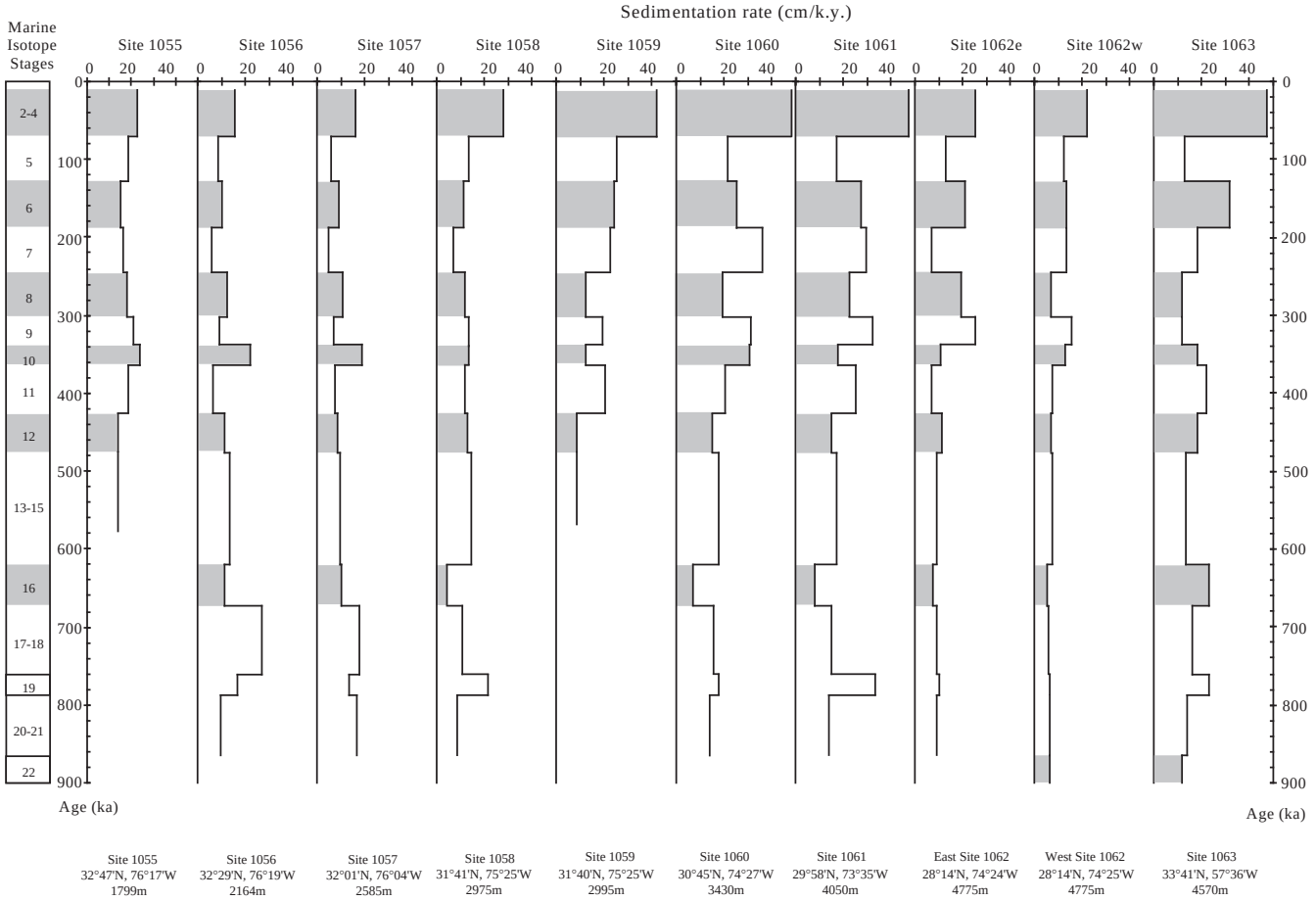

Figure 4. Sedimentation rates for Sites 1055 through 1063, based on the marine isotopic stage chronology developed in Figure 3. Note the generally higher rates for the latest Pleistocene, and the higher rates at deeper sites.

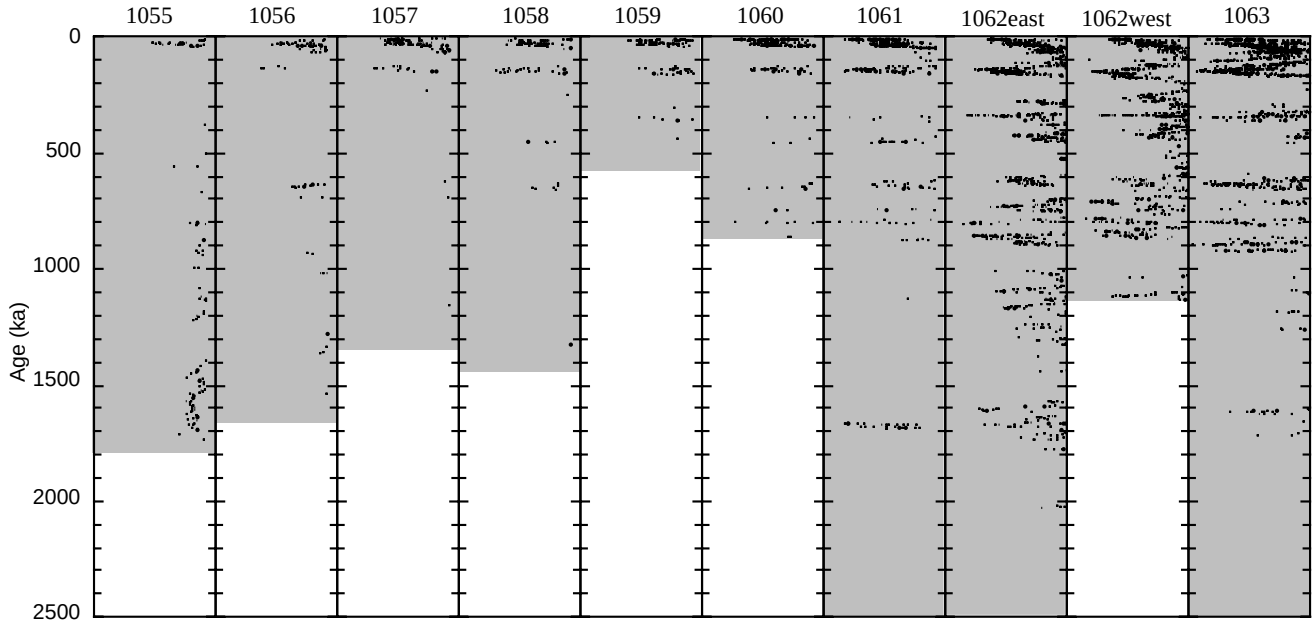

Figure 5. Distribution of red lutites at Sites 1055 through 1063, based on color reflectance. Red color increases from right to left in each site graph, and the gray pattern at each site represents the cored interval (2500 ka). For 1062west, only information from Hole 1062F has been included. The abscissa for each site ranges from 0° (left) to 80° (right) in hue-saturation value space.

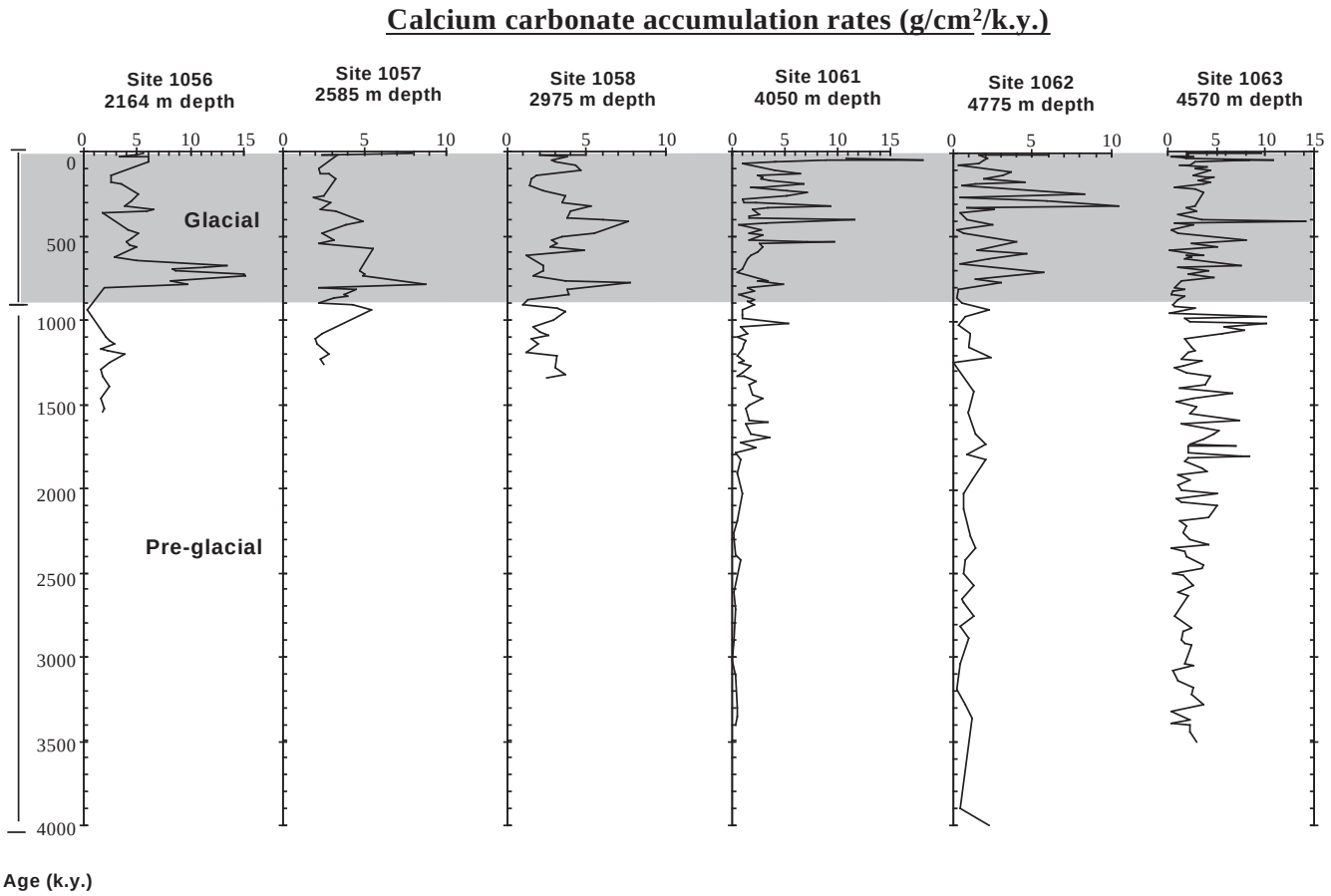

Figure 6. Mass accumulation rates of calcium carbonate at selected Leg 172 sites. Note the suggestion of higher and more variable carbonate accumulation in sediments younger than ~0.9 Ma.

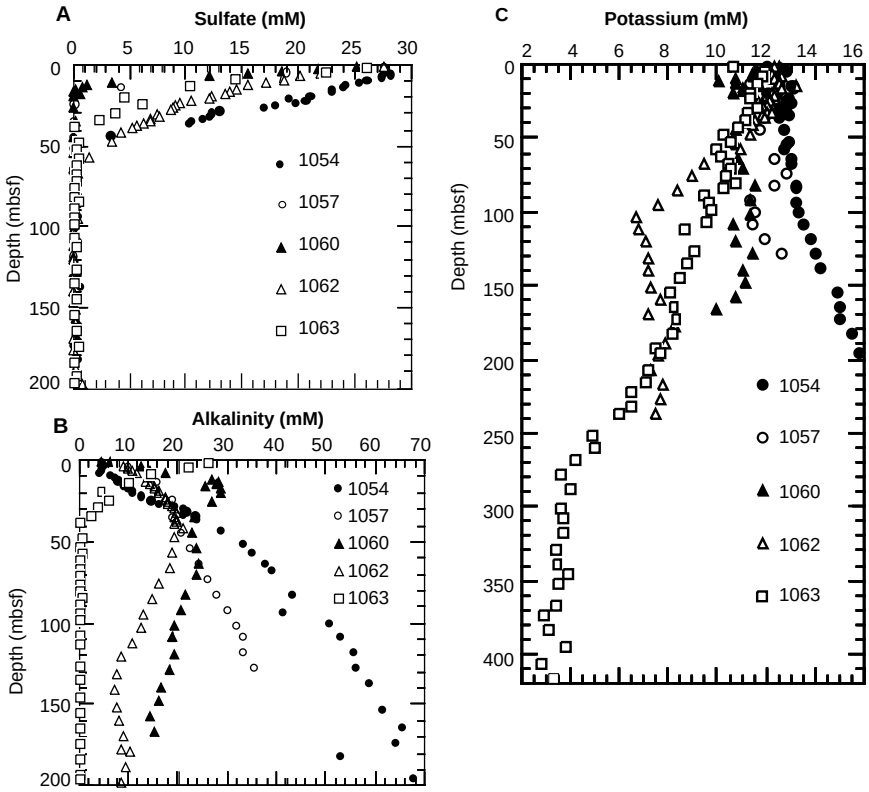

Figure 7. (**A**) Pore-water sulfate, (**B**) alkalinity, and (**C**) potassium at selected Leg 172 sites.

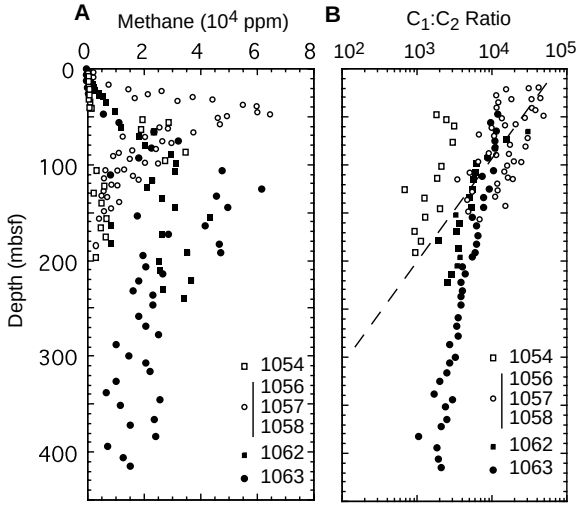

Figure 8. (**A**) Methane concentration and (**B**) methane/ethane ratios (C_1/C_2) for selected Leg 172 sites. Sites 1056–1058 are grouped together and indicated by an open circle.

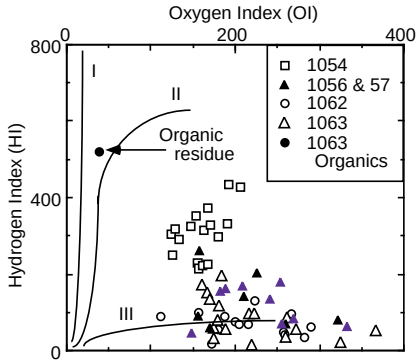

Figure 9. Rock-eval van Krevelen-type diagram of selected Leg 172 sites. Hydrogen index = mg hydrocarbons/g organic carbon, Oxygen index = mg CO_2/g organic carbon. The curves I, II, and III refer to trends of three types of organic matter: type I = algal, oil-prone organic matter; type II = marine, oil/gas-prone organic matter; and type III = terrestrial, gas-prone organic matter.

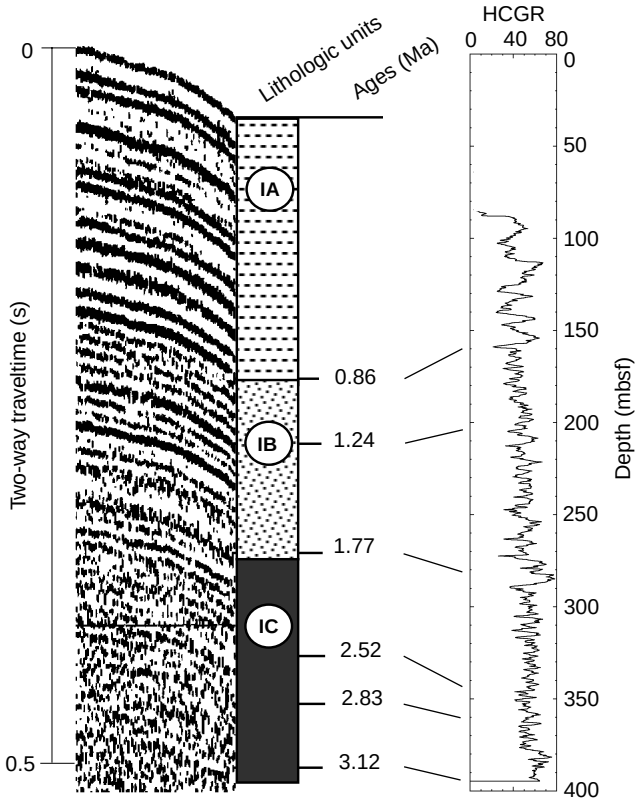

Figure 10. Comparison of 3.5-kHz reflectors, lithostratigraphy (Subunits 1A, 1B, and 1C), chronology based on magnetostratigraphy and biostratigraphy, and HCGR log results (see Fig. 11) from Bermuda Rise Site 1063. Note the first occurrence of distinctive reflectors close to the Pliocene/Pleistocene boundary (1.86 Ma), and the change to less frequent but more distinctive reflectors at ~0.86 Ma.

dence of this event is found on the Bermuda Rise. To a depth of 0.20 s two-way traveltime the reflectors in the seismic profile at Site 1063 are of high amplitude and low frequency (Fig. 10). At this depth an abrupt transition occurs: the deeper reflectors become slightly lower in amplitude and are much more closely spaced, that is, they have a higher frequency. Preliminary analysis of the interval velocity of the sediments using the well-logging measurements at Site 1063A suggests that this transition from low-frequency (widely spaced) to high-frequency (closely spaced) reflectors is at ~162 mbsf. Stratigraphic analysis at Site 1063 places this depth at ~0.86 Ma, very close to the switchover from climate dominated by 100-k.y. orbital forcing to climate dominated by 40-k.y. forcing. This transition and these cycles can also be seen in the bulk density measurements derived from the gamma-ray attenuation porosity evaluator at Site 1063. The properties of sediments younger than 0.86 Ma vary, with conspicuously longer wavelengths than those of older sediments.

The "mid-Pleistocene transition" is particularly well documented by logging results at Sites 1061 and 1063, and the degree of similarity between such distant sites (Fig. 1) lends credence to the existence of an underlying but still unknown cause. Figure 11 compares the older 100 k.y.-cycles of (1) SPECMAP, (2) the hostile environment computed gamma-ray (HCGR) log from Site 1063, and (3) the resistivity logs (IMPH) of Sites 1061 and 1063, after adjustment of the depth scale of Site 1061 to correlate with that at Site 1063. The logs are characterized by long-wavelength cycles that contrast with shorter cycles of lesser amplitude below 162 mbsf. Clearly the logs are tracking the older 40-k.y. and the younger 100-k.y. climate cycles.

The resistivity and natural gamma radiation logs follow the known glacial–interglacial stages of the MIS record ($\delta^{18}O$; Fig. 11). MIS 19 is pinned by the B/M boundary to 138.5 mbsf, and MIS 12 by the LO of *P. lacunosa* at 95.8 mbsf; between these tie points the pattern of the logs closely matches the pattern of isotope stages. The shape of the glacial and interglacial cycles matches as well. Note that glacial MISs 16 and 22 are more prominent than the others in both the SPECMAP stack and the logs. Peaks in natural gamma radiation are a measure of clay content (because the potassium and thorium that emit the gamma rays are mostly in the clays) and the glacial sediment has a higher clay content than the interglacial sediment.

It was speculated before coring that the acoustical lamination of the sediment on the Bermuda Rise was the result of a change in physical properties associated with the origin of Northern Hemisphere glaciation. However, it now seems clear that the reflective sediments are much younger. Results of drilling at Site 1063 show that the seismically high-amplitude (bright) sediments of the northern Bermuda Rise have accumulated continuously since about 1.5 Ma (Fig. 10). The reflectors older than 1.5 Ma are much lower amplitude and fade gradually with depth until they are barely noticeable at 2.52 Ma. This suggests that, although the onset of Northern Hemisphere glaciation contributed large volumes of sediment to the northern Bermuda Rise and the sedimentation rates were high, the onset itself did not create the seismically bright sediments. The influence of the climatic system on the seismic characteristics on the sediments of the northern

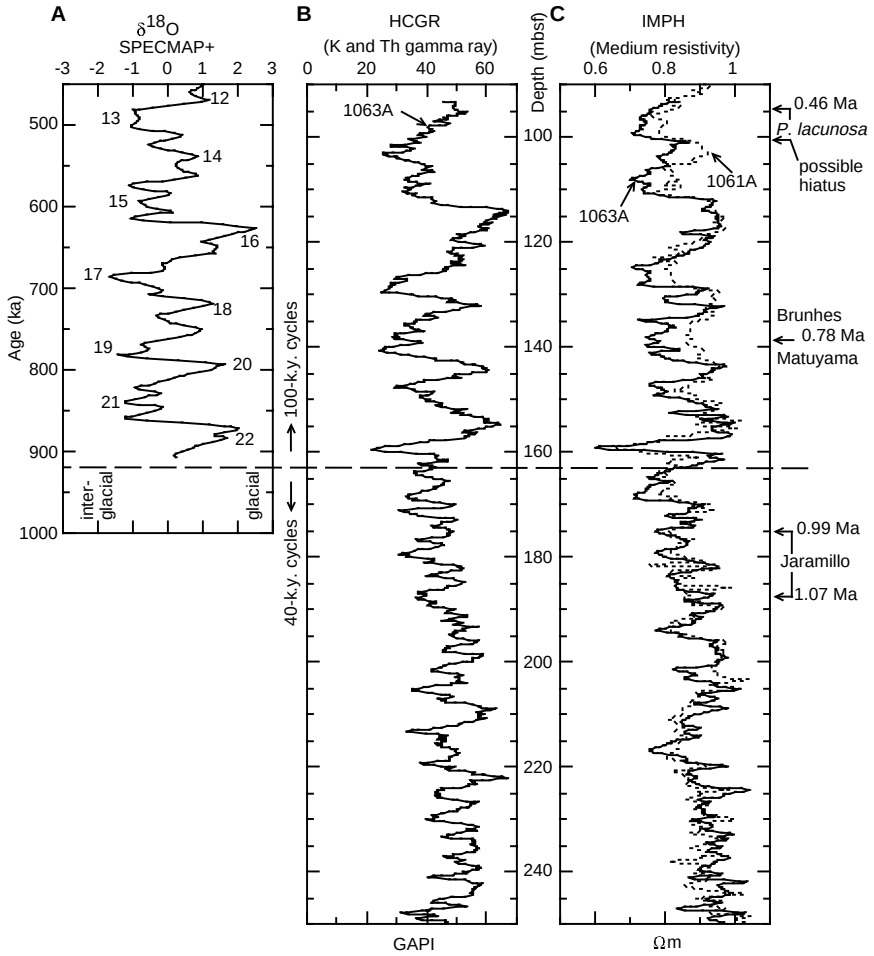

Figure 11. Comparison of (**A**) the generalized SPECMAP oxygen isotope stratigraphy and (**B**) HCGR log results from Bermuda Rise Site 1063 with (**C**) IMPH log results from Blake Outer Ridge Site 1061 scaled to results from Site 1063. Note the striking change in downhole properties at ~0.86 Ma and the coherence of these properties with the SPECMAP ice volume proxy.

Bermuda Rise must have evolved over time until about 1.5 Ma, when conditions were right to create seismically well-stratified sediments.

From 1.5 Ma to 0.86 Ma the climatic system imparted a 40-k.y. variability to the stratigraphic section and, thereby, to the seismic records. At 0.86 Ma the switchover to 100-k.y. cycles began to leave its mark. Determining the reasons for these changes will require further study.

PRELIMINARY PALEOMAGNETIC RESULTS

The Leg 172 cores contain perhaps the most detailed and complete record ever recorded of the Earth's magnetic field variability for the past 1.2 Ma. Replicate records of magnetic field secular variation (both directions and intensity) have been recovered using onboard long-core natural remanent magnetization (NRM) measurements. At least 14 Brunhes-aged excursions (Figs. 12, 13) and at least four Matuyama-aged excursions are found within the secular variation. We have also recovered magnetic-field transition records for the Brunhes/Matuyama (Fig. 14), Jaramillo onset/termination, and Cobb Mountain onset/termination boundaries. These records of magnetic field behavior are all in sediments with accumulation rates between 10 and 25 cm/k.y. and they provide a great opportunity to resolve details of magnetic field variability that have not previously been recovered from ODP sediment sequences. Finally, we have recovered replicate paleomagnetic reversal polarity stratigraphies that span the Brunhes to Gauss Chrons (0–3.2 Ma) and contain clear evidence for the Cobb Mountain and two Reunion Events.

Directional records of secular variation could commonly be correlated between holes at individual sites for Sites 1060–1063 and between sites over more than 1600 km from the Blake Outer Ridge (Sites 1060 and 1061) to the Bahama Outer Ridge (Site 1062) and the Bermuda Rise (Site 1063) (Fig. 12; Table 1). Short-duration (10^3 yr), secular variation features identified in the 0- to 200-ka record (MISs 1–6) were also correlatable with previously published studies from the same region. Selected longer duration features (10^4–10^5 yr), could also be correlated between sites primarily in the inclination records. Such features are interpreted to indicate deviations in the normal process of local secular variation. Intensity records of magnetic-field secular variation were also estimated based on normalization of long-core NRM intensities (20 mT alternating field [AF] demagnetization) by long-core–measured magnetic susceptibility. The initial results are broadly consistent with previously published records of Brunhes magnetic-field intensity variation.

Our onboard paleomagnetic measurements indicate that at least 14 magnetic field excursions have occurred over the last 780 k.y. during a time of apparently stable normal magnetic-field polarity (Brunhes Epoch). Most of the excursions tend to occur in "bundles" of two or three with intervening intervals of distinctive magnetic field secular variation. Altogether, the bundles tend to span 20–50 k.y. It is possible that these bundles of closely spaced excursions indicate a continuing "excursional state" or pattern in the core dynamo process that exists for the duration of the bundles. The number and ages of our Brunhes excursions also suggests that excursions can no longer be viewed as simply or even primarily regional anomalies of the geomagnetic field. Within one small region, we have identified more Brunhes-aged excursions than all previously high-quality paleomagnetic studies worldwide put together. Moreover, the ages of our excursions are not significantly different from any of the previously identified high-quality excursions from around the world. If confirmed by further discrete and u-channel measurements, then all of these observations suggest that excursions are not rare, random per-

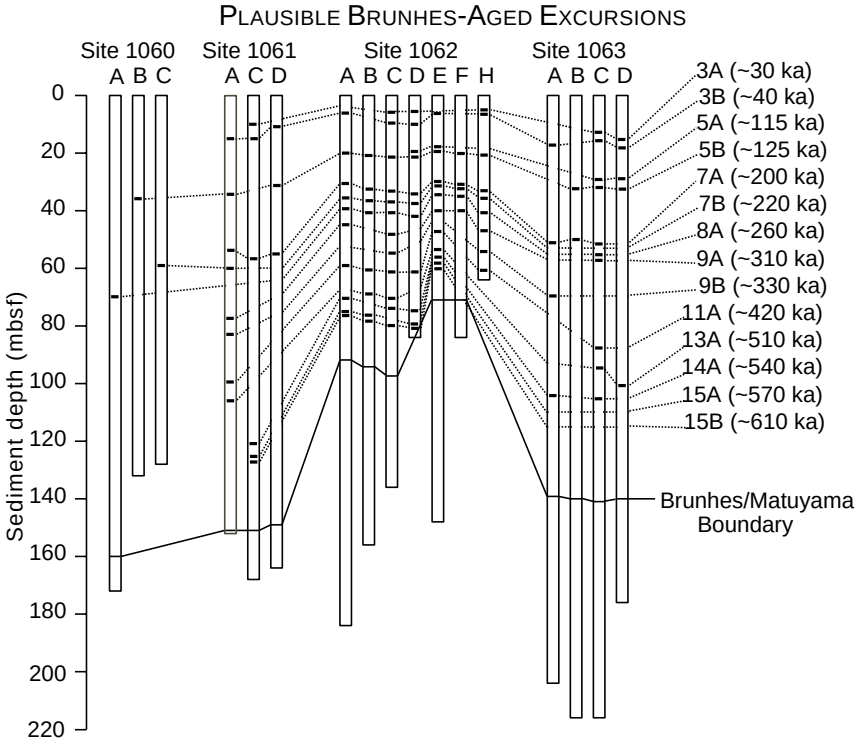

Figure 12. Distribution of plausible Brunhes-aged paleomagnetic excursions among holes at Sites 1060–1063. Excursions are considered "plausible" if they occur in more than one hole in at least two sites.

turbations of the stable geomagnetic field, but rather an important systematic and distinct component of the Earth's magnetic field variability between field reversals.

Replicate magnetic-field-reversal transition records have also been recovered for the B/M, Jaramillo onset/termination, and Cobb Mountain onset/termination boundaries. Initial long-core and discrete measurements of the B/M transition indicate that a fast polarity change occurs in only ~1000 yr or less, and there are perhaps three magnetic field excursions within 10 k.y. before the transition and perhaps two excursions within 10 k.y. afterward. Whether these excursions constitute pre- and post-transitional field behavior or are an intrinsic part of the transition are topics for future study.

COMPARISON OF THE BRUNHES/MATUYAMA POLARITY TRANSITION RECORDED AT SITES 1060 AND 1063

Understanding how and why Earth's magnetic field reverses polarity remains a major unsolved mystery in geophysics. Paleomagnetic records of the changes that occur in the field as it reverses are our only source of information about how the reversal process occurs. However, reversals are nearly instantaneous on geologic time scales, taking between 4 and 8 k.y. to occur. For this reason, it has proven difficult to obtain high-resolution transition records, and considerable doubt exists concerning the accuracy of transition records obtained from low deposition-rate sediments. The high sedimentation-rate cores from Leg 172 provide an important opportunity to examine geomagnetic field variability, including polarity reversal transitions on a range of temporal scales.

Detailed measurements of the B/M polarity transition were made using both discrete sample and long-core methods at several sites cored during Leg 172. The results, such as the comparison of inclinations spanning the reversal recorded in Holes 1060A and 1063D, exhibit a remarkable degree of similarity (Fig. 14). This is an extremely important step toward demonstrating the reproducible nature of magnetizations acquired while the geomagnetic field was very weak and possibly changing rapidly. These two holes were cored at locations that are close enough for us to expect similar directional changes to occur during a reversal even if the transitional field was largely nondipolar. However, they are far enough apart that the sedimentary processes that may have affected the remanence acquisition process should differ. The directions recorded through this reversal occur during a low in relative paleointensity and pass through a very steeply downward pointing interval, consistent with the virtual geomagnetic pole passing close to these sites during the reversal.

PRELIMINARY BIOSTRATIGRAPHIC RESULTS

A detailed calcareous nannofossil biostratigraphy was obtained by shipboard analyses. The fossil assemblages were generally rich, with nannofossils mostly well preserved and abundant. In some cases, sedimentological processes, such as redeposition, affected the integrity of the biostratigraphic signal, but it never seriously hindered the biostratigraphic classification. In the sedimentary successions drilled on the Carolina Slope and at the shallower sites on the Blake-Bahama Outer Ridge, the nannofossils were sometimes strongly reduced in numbers through "dilution" by terrigenous input (biogenic fragments and clay particles), but preservation remained good, and the biostratigraphic characterization of those sediments was always possible. Only in the few intervals affected by downslope transport processes were there inconsistencies in the nannofossil record.

At the deeper sites (Sites 1060 to 1062)—despite the presence of some intervals with strong dissolution, dilution by terrigenous input, and noise produced by reworking—the observed nannofossil assemblages preserved the biostratigraphic series of nannofossil marker species. In most of the Pleistocene interval the biochronologic framework was provided by a well-established and calibrated succession of biohorizons (Fig. 2) that mainly relies on a taxonomic subdivision of the gephyrocapsids (see Raffi et al., 1993). Only two late Pleistocene nannofossil biohorizons were not detected. The interval of *E. huxleyi* dominance and the first appearance datum (FAD) of *E. huxleyi* are recognizable only with the scanning electron microscope. All the late to early Pliocene biohorizons were recognized.

The availability of reliable magnetic susceptibility stratigraphy in most of the sections recovered often allowed a preliminary age correlation of the nannofossil datums, which generally confirmed the va-

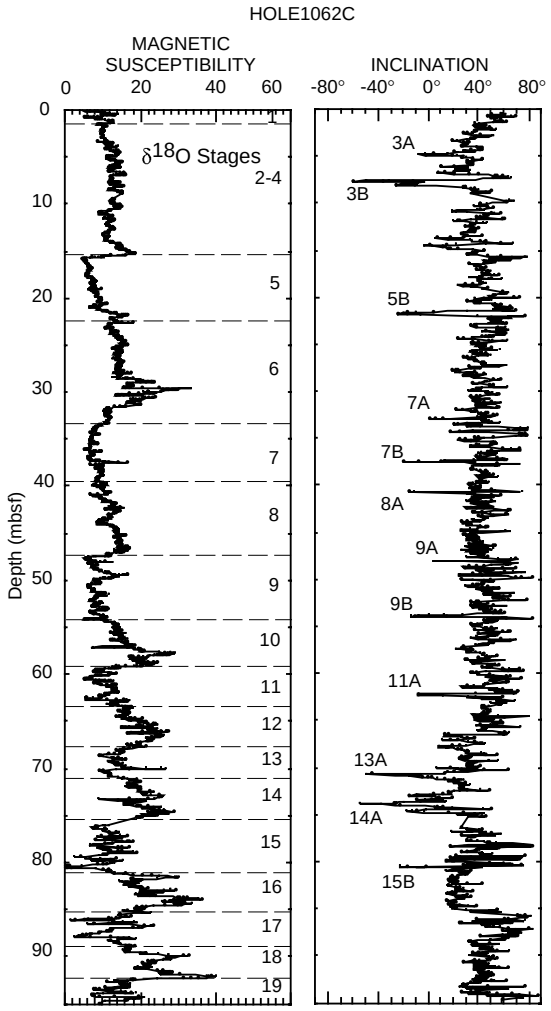

Figure 13. Example of occurrence of plausible excursions at Bahama Outer Ridge Hole 1062C.

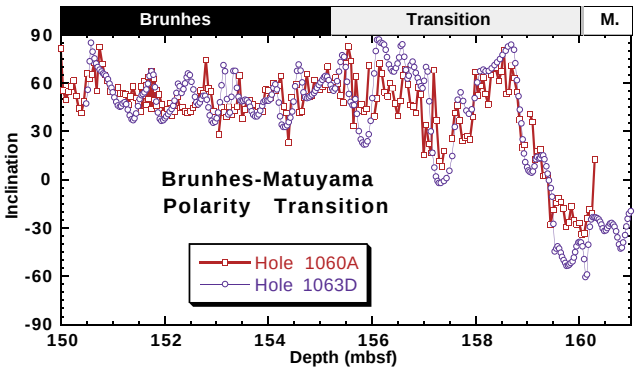

Figure 14. Example of the high-resolution record of the Brunhes/Matuyama transition at Holes 1060A and 1063D.

lidity of the biochronologic scheme used. The high quality (in terms of high sedimentation rates and good nannofossil assemblages) of the recovered sedimentary successions will provide the opportunity to further test with a high degree of precision the biochronology of some nannofossil biohorizons in both the Pleistocene and Pliocene intervals. Moreover, there will be opportunity to investigate in detail the influence of changing paleoceanographic conditions on the nannofossil assemblages.

Table 1. Summary of identified and plausible Brunhes excursion records, Sites 1060, 1061, 1062, and 1063.

Identified excursion	Number of sites	Number of holes	General age (ka)
3A	3	6	30
3B	3	11	40
5A	2	4	115
5B	4	13	125
7A	3	12	200
7B	3	9	220
8A	3	9	260
9A	3	7	310
9B	3	4	330
11A	3	7	420
12A	1*	1*	
13A	3	6	510
14A	3	7	540
15A	2	5	570
15B	2	6	610
17A	1*	1*	

Plausible excursions identified at individual sites

Site 1060 (N = 3): 5B, 7B, 8A

Site 1061 (N = 12): 3A, 3B, 5B, 7A, 7B, 9A, 9B, 11A, 13A, 14A, 15A, 15B

Site 1062 (N = 14): 3A, 3B, 5A, 5B, 7A, 7B, 8A, 9A, 9B, 11A, 13A, 14A, 15A, 15B

Site 1063 (N = 11): 3A, 3B, 5A, 7A, 8A, 9A, 9B, 11A, 13A, 14A

Note: * = questionable results.

In contrast to the nannofossils, planktonic foraminifer numbers were often reduced by dissolution and dilution at all sites deeper than Site 1059. However, intervals of surprisingly good preservation were found during interglacials at the deeper sites. In addition, the calibrations of the Pleistocene foraminifer datums do not seem to be as accurate as those of the nannofossils. Berggren et al. (1995) published tables of Pleistocene and Pliocene planktonic foraminifer datums that were calibrated to the tuned time scales of Shackleton et al. (1995) and Hilgen (1991a, 1991b), and in several cases they tabulated the coeval MISs. For Leg 172 work these datum ages were updated to agree with the time scale of Lourens et al. (1996). We plotted the depths of biohorizons against the record of magnetic susceptibility for at least one hole per site. Assuming that this record is roughly an inversion of the oxygen isotope record for the Pleistocene (SPECMAP), our initial results indicate that the calibrations of Berggren et al. (1995) for planktonic foraminifer datums may either need further work or the datums are diachronous. Nannofossil datums, by contrast, seem either well calibrated or can be shown to be systematically diachronous.

The following is an incomplete list of some of the apparent discrepancies between the Leg 172 record and the published ages. The of LO *Globorotalia tumida flexuosa* (0.068 Ma) seems consistently too old, falling in MIS 5 instead of in MIS 4. Furthermore, the FO of this species (0.401 Ma) in MIS 11 (Berggren et al., 1995) is actually a reentrant. Good specimens of *G. tumida flexuosa* were found in MIS 19 and in the early Pleistocene, suggesting that this form appears during interglacials throughout the Pleistocene. The FOs of *Globigerinella calida* (0.22 Ma) and *Hirsutella hirsuta* (0.45 Ma) could not be constrained because typical specimens of these species were observed only episodically throughout the Pleistocene at the shallower BBOR sites. However, at nearly all Leg 172 sites the *H. hirsuta* record included a consistent reentrant event just above the *G. tumida flexuosa* reentrance in MIS 11. The FO of *Truncorotalia crassaformis hessi* (0.75 Ma) may also be a reentrant, but the taxonomy of this variety will have to be more specifically described before early Pleistocene and late Pliocene specimens found at several sites can be accepted. Finally, *Menardella miocenica* appears to go extinct before 2.3 Ma, possibly at the BBOR, and more definitely at Bermuda Rise.

The unusually high sediment accumulation rates at the BBOR may have made it easier to find brief reentrants, such as those of *G. tumida flexuosa* and *T. crassaformis hessi.* But the other discrepancies are more likely to be diachronies that result from early retreat of species from the subtropics before extinction. The generation of

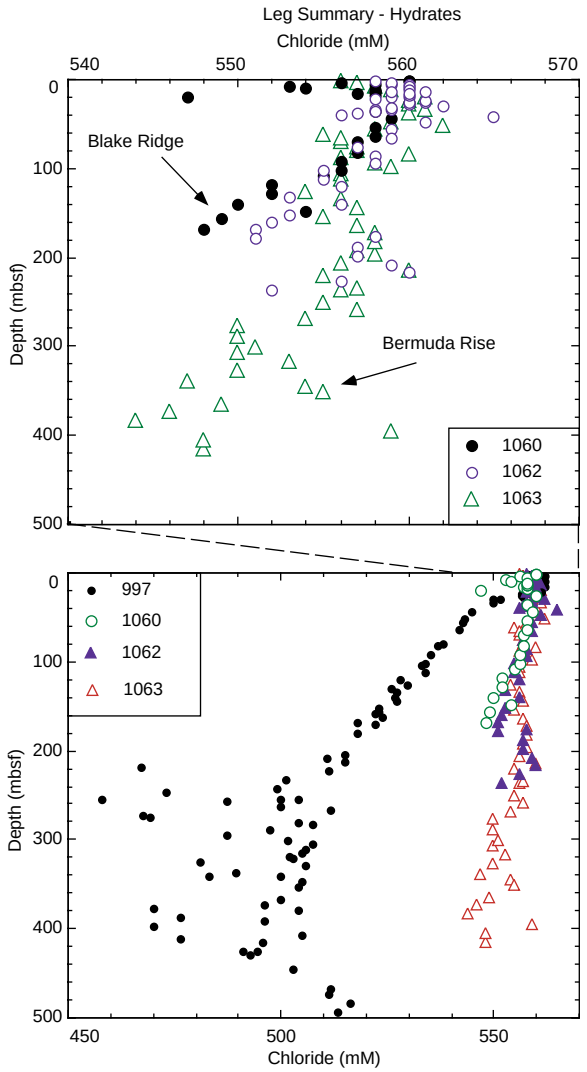

Figure 15. Pore-water chloride at BBOR Sites 1060 and 1062, and at Bermuda Rise Site 1063, compared to Blake Outer Ridge Site 997 (Site 997 data are from Shipboard Scientific Party, 1996). Decreasing chloride concentration with depth at Leg 172 sites suggests the presence of gas hydrate.

high-resolution isotope records at a number of Leg 172 sites will make better North Atlantic calibration of these datums possible.

Finally, diatoms were found in a large number of core-catcher samples at many Leg 172 sites. On the Bermuda Rise (Site 1063), greater numbers of diatoms were associated with low bulk density and magnetic susceptibility values. This seems to be a production rather than a preservation phenomenon, as other siliceous microfossils were observed in intervening samples.

GEOGRAPHIC EXTENT OF GAS HYDRATE

Leg 172 research has greatly increased the documented extent of gas hydrate underlying the BBOR, the best-known occurrence of continental margin gas hydrate in the world. Gas hydrate occurrence is typically inferred by mapping the presence of bottom-simulating reflectors (BSRs), and by noting decreased chlorinity in pore waters that can result from the melting of hydrate during core recovery. BSRs and downward-freshening chloride profiles were found at every site on the BBOR, which extends the known occurrence of gas hydrate to waters 1000 m deeper than they have been previously found (Dillon and Paull, 1983).

Gas hydrate may even exist on the Bermuda Rise, which, if true, would be the first known occurrence in an oceanic setting (Kvenvolden, 1988; Kvenvolden et al., 1993). There is no BSR near Site 1063, but chloride systematically freshens by 3% compared to bottom water over the length of the hole (Fig. 15). Other possible causes of decreased chloride concentrations (meteoric water, water released from hydrous minerals, and ion filtration by clays; see "Inorganic Geochemistry" section, "Bermuda Rise and Sohm Abyssal Plain" chapter, this volume) seem unlikely. Provided onshore studies eliminate these other possibilities, the remaining explanation for decreased chloride concentration is that gas hydrate lies at depth within the Bermuda Rise. If significant numbers of other localities exist with the correct interplay of adequate amounts of organic carbon, low geothermal gradients, deep water, and relatively thin sedimentary sequences, then the occurrence of gas hydrate may be more widespread than expected. Thus, even larger amounts of methane and carbon may be stored in gas hydrate than previously estimated (e.g., Kvenvolden, 1988).

REFERENCES

Barranco, F.T., Jr., Balsam, W.L., and Deaton, B.C., 1989. Quantitative reassessment of brick red lutites: evidence from reflectance spectrophotometry. *Mar. Geol.*, 89:299–314.

Berggren, W.A., Hilgen, F.J., Langereis, C.G., Kent, D.V., Obradovich, J.D., Raffi, I., Raymo, M.E., and Shackleton, N.J., 1995. Late Neogene chronology: new perspectives in high-resolution stratigraphy. *Geol. Soc. Am. Bull.*, 107:1272–1287.

Berner, R.A., 1980. *Early Diagenesis: A Theoretical Approach:* Princeton, NJ (Princeton Univ. Press).

Dillon, W.P., and Paull, C.K., 1983. Marine gas hydrates, II. Geophysical evidence. *In* Cox, J.L. (Ed.), *Natural Gas Hydrates: Properties, Occurrences, and Recovery:* Woburn, MA (Butterworth), 73–90.

Hilgen, F.J., 1991a. Astronomical calibration of Gauss to Matuyama sapropels in the Mediterranean and implication for the geomagnetic polarity time scale. *Earth Planet. Sci. Lett.*, 104:226–244.

————, 1991b. Extension of the astronomically calibrated (polarity) time scale to the Miocene/Pliocene boundary. *Earth Planet. Sci. Lett.*, 107:349–368.

Kvenvolden, K.A., 1988. Methane hydrate—a major reservoir of carbon in the shallow geosphere? *Chem. Geol.*, 71:41–51.

Kvenvolden, K.A., Ginsburg, G.D., and Solovyev, V.A., 1993. Worldwide distribution of subaquatic gas hydrates. *Geo-Mar. Lett.*, 13:32–40.

Lourens, L.J., Antonarakou, A., Hilgen, F.J., Van Hoof, A.A.M., Vergnaud-Grazzini, C., and Zachariasse, W.J., 1996. Evaluation of the Plio-Pleistocene astronomical timescale. *Paleoceanography*, 11:391–413.

Mackin, J.E., and Aller, R.C., 1984. Ammonium adsorption in marine sediments. *Limnol. Oceanogr.*, 29:250–257.

Pedersen, T.F., and Shimmield, G.B., 1991. Interstitial water chemistry, Leg 117: contrasts with the Peru Margin. *In* Prell, W.L., Niitsuma, N., et al., *Proc. ODP, Sci. Results*, 117: College Station, TX (Ocean Drilling Program), 499–513.

Raffi, I., Backman, J., Rio, D., and Shackleton, N.J., 1993. Plio-Pleistocene nannofossil biostratigraphy and calibration to oxygen isotopes stratigraphies from Deep Sea Drilling Project Site 607 and Ocean Drilling Program Site 677. *Paleoceanography*, 8:387–408.

Rosenfeld, J.K., 1979. Ammonium absorption in nearshore anoxic sediments. *Limnol. Oceanogr.*, 24:356–364.

Shackleton, N.J., Crowhurst, S., Hagelberg, T., Pisias, N.G., and Schneider, D.A., 1995. A new late Neogene time scale: application to Leg 138 sites. *In* Pisias, N.G., Mayer, L.A., Janecek, T.R., Palmer-Julson, A., and van Andel, T.H. (Eds.), *Proc. ODP, Sci. Results*, 138: College Station, TX (Ocean Drilling Program), 73–101.

Shipboard Scientific Party, 1996. Site 997. *In* Paull, C.K., Matsumoto, R., Wallace, P.J., et al., *Proc. ODP, Init. Repts.*, 164: College Station, TX (Ocean Drilling Program), 277–334.

Ms 172IR-107

Prior Chapter Contents Next Chapter